

## ORIGINAL ARTICLE

Food Engineering, Materials Science, and Nanotechnology

# Innovative chitosan-onion polysaccharide composite films: A study on the preservation effects on cherry tomatoes

Ao Shen<sup>1</sup> | Tianzhu Zhang<sup>2,3</sup> | Shuzhen Li<sup>4</sup> | Miaorong Xiao<sup>1</sup> | Zhijun Tian<sup>1</sup> | Jin Zhang<sup>1</sup> | Tongtong Lu<sup>1</sup> | Weiwei Yang<sup>1</sup> 

<sup>1</sup>Department of Food Science, College of Public Health, Shenyang Medical College, Shenyang, China

<sup>2</sup>College of Pharmacy, Chongqing Medical and Pharmaceutical College, Chongqing, China

<sup>3</sup>Chongqing Engineering Research Center of Pharmaceutical Sciences, Chongqing, China

<sup>4</sup>Department of Immunology, College of Basic Medical Sciences, Shenyang Medical College, Shenyang, China

**Correspondence**

Weiwei Yang, Department of Food Science, College of Public Health, Shenyang Medical College, Shenyang 110034, China.

Email: yangweiwei@symc.edu.cn

**Funding information**

Shenyang Medical College Scientific Research Innovation Fund, Grant/Award Numbers: 20182033, 20191038; Natural Science Foundation of Liaoning Province, Grant/Award Numbers: 2018010874-301, 2017225065

**Abstract:** Natural preservation materials have long been a focus of research in the quality control of fruits and vegetables. This study aimed to develop composite films with exceptional preservation properties by utilizing chitosan (CS) as the film-forming material and incorporating onion polysaccharide (ONP) as the active component. The CS-ONP composite films were prepared, and their performance and preservation effects were evaluated. The results demonstrated that increasing the ONP content significantly enhanced the shading, antimicrobial, and antioxidant capabilities of the CS-ONP composite films. Preservation experiments revealed that the CS-ONP composite films effectively delayed the quality decline of cherry tomatoes during storage. However, despite the improvements brought by ONP, certain drawbacks persisted, such as reduced mechanical properties and alterations in surface structure. In summary, the CS-ONP composite films exhibit promising potential as novel materials for fruit and vegetable preservation.

**KEYWORDS**

cherry tomatoes, chitosan, composite films, onion polysaccharide, preservation efficacy

**Practical Application:** The spoilage of fruits and vegetables can cause huge economic losses. This study addresses this challenge by using chitosan as the film-forming substrate and adding crude onion polysaccharide as the active ingredient to create composite films. The preservation effects of these films on cherry tomatoes were studied. Although only cherry tomatoes were tested in this study, the composite films demonstrated significant potential for broader applications in fruit and vegetable preservation.

## 1 | INTRODUCTION

Polysaccharides have demonstrated considerable potential in the preservation of fruits and vegetables. Our previous study identified significant antimicrobial and preservation

capabilities in polysaccharide extracted from *Pleurotus citrinopileatus* (Shen et al., 2023). Building on this discovery, we further explored the efficacy of other polysaccharides. Onion polysaccharide (ONP) is composed of various monosaccharides joined by  $\alpha$ -glycosidic bonds, including fucose, arabinose, rhamnose, glucose, mannose, xylose, and galactose (Kumari et al., 2022; Wilson et al., 2021;

Ao Shen, Tianzhu Zhang, and Shuzhen Li are contributed equally to this work.

Zhou, Huang, et al., 2022). Recent research has primarily focused on the biological functions of ONP. For instance, Zhou's study demonstrated that ONP can enhance lipid metabolism, reduce blood glucose levels, alleviate liver and kidney damage, and increase the rate of scavenging free radicals such as DPPH, thus manifesting antioxidative properties (Zhou, Zhao, et al., 2022). The limited studies on the application of ONP highlight the practical significance of this research.

Chitosan (CS), an alkaline polysaccharide, is widely recognized as a biodegradable film material due to its exceptional film-forming properties (Abd El-Hack et al., 2020; Cohen & Poverenov, 2022). Despite its intrinsic antimicrobial and antioxidant capabilities, CS films alone often fail to achieve satisfactory outcomes in practical applications. This shortcoming is attributed to the slow diffusion rate of CS molecules within the films (Matica et al., 2019). Consequently, it is common practice to introduce supplementary components during the preparation of CS films to overcome this limitation and achieve the desired film characteristics. For example, the addition of xanthan gum enhances the mechanical properties of CS films, whereas the inclusion of plant essential oils improves their antimicrobial and antioxidant capabilities (de Moraes Lima et al., 2017). However, research on CS-plant polysaccharide composite films remains significantly limited.

This study aims to integrate ONP into the fabrication process of CS films, resulting in the development of CS-ONP composite films. The performance of these composite films will be comprehensively examined. Additionally, the application value of these composite films will be preliminarily evaluated by observing their effects on the preservation of cherry tomatoes.

## 2 | MATERIALS AND METHODS

### 2.1 | Materials

ONP (50% purity) and CS were purchased from Waters Bio-Tech Co., Ltd. Cherry tomatoes (variety: Millennium) were obtained from a local farmers' market (Shenyang, China). *Escherichia coli*, *Pseudomonas aeruginosa*, *Bacillus subtilis*, *Bacillus cereus*, *Aspergillus flavus*, *Aspergillus niger*, *Botrytis cinerea* Pers, and *Penicillium expansum* were obtained from the China General Microbiological Culture Collection Center. Brain–heart infusion broth (BHI) and nutrient agar were purchased from Ze Ye Biotech Co., Ltd. All other reagents used were of analytical grade.

### 2.2 | Preparation of films

In a beaker, 100 mL of a 2% acetic acid solution, 1 mL of glycerol, and 3 g of CS were combined and stirred magnetically (DF-101S Magnetic Stirrer, YuHua Instrument) until fully dissolved. Subsequently, ONP was added in varying amounts of 50, 100, 150, and 200 mg, with continuous stirring to ensure uniform mixing. A control group was prepared without the addition of ONP (0 g/L polysaccharide concentration), whereas four other groups were established with ONP concentrations of 0.5, 1, 1.5, and 2 g/L. The homogenized solutions were subjected to ultrasonic vibration (YH-200DH Ultrasonic Cleaner, YuHao Scientific Instrument) to remove bubbles and then spread onto 25 cm × 25 cm glass plates. The glass plates were placed in an oven (DHG9070A Oven, YiHeng Scientific Instrument) and dried at 60°C for 6 h. After drying, the plates were removed, cooled to room temperature, and the films were carefully peeled off. The films were then left to rest for 24 h under ambient conditions (temperature: 25°C; relative humidity: 60%) before subsequent testing.

### 2.3 | Determination of film properties

#### 2.3.1 | Determination of thickness, color difference ( $\Delta E$ ), and transmittance ( $T$ )

The thickness of the films was measured using a thickness gauge (CHY-CA, SaiCheng Instrument) with a sensitivity of 0.01 mm. Measurements were taken at six different points on each film.

The color difference of the films was measured using a colorimeter (NR20XE, 3NH Technology). Prior to measurement, the device was calibrated using a standard white tile ( $L = 93.28$ ,  $a = -1.1$ ,  $b = -1.3$ ). Measurements were taken at three different positions on each film, and values for  $L^*$  (brightness),  $a^*$  (red/green), and  $b^*$  (yellow/blue) were recorded. The total color difference ( $\Delta E$ ) was calculated using the following formula:

$$\Delta E = \left[ (L^* - L)^2 + (a^* - a)^2 + (b^* - b)^2 \right]^{0.5}$$

A 10 mm × 40 mm film sample was used to measure the transmittance in the range of 200–800 nm using a UV–visible spectrophotometer (Evolution 201, Thermo Fisher Scientific).

### 2.3.2 | Determination of moisture content (MC), swelling degree (SD), water solubility (WS), and water vapor permeability (WVP)

Initially, a 20 mm × 20 mm film sample was taken, and its initial weight was recorded as  $m_1$ . The film was then dried at 105°C for 24 h in an oven, and its weight was recorded as  $m_2$ . Subsequently, the dried film was placed in a beaker containing 50 mL of distilled water and sealed with plastic wrap. After 24 h, the film was removed, surface moisture was wiped off, and its weight was recorded as  $m_3$ . Finally, the water-immersed film was dried again at 105°C for 24 h, and its weight was measured and recorded as  $m_4$ . The moisture content, swelling degree (SD), and water solubility of the films were calculated using the following formulas:

$$MC (\%) = \frac{m_1 - m_2}{m_1} \times 100\%$$

$$SD (\%) = \frac{m_3 - m_2}{m_2} \times 100\%$$

$$WS (\%) = \frac{m_2 - m_4}{m_2} \times 100\%$$

For determining water vapor permeability (WVP), 50 mL of distilled water was added to a 100 mL beaker, and the beaker's opening was sealed with the film. The beaker was then placed in a desiccator (relative humidity: 20%). The total weight of the beaker, distilled water, and film was measured at various time points every 8 h over a 24-h period. The water vapor transmission rate was calculated using the following formula:

$$WVP = \frac{G \times L}{t \times s \times \Delta P}$$

where  $G$  represents the total weight change (g),  $L$  represents the film thickness (mm),  $t$  represents the time interval (s),  $s$  represents the area of the beaker mouth (mm<sup>2</sup>), and  $\Delta P$  represents the water vapor pressure difference across the film (3168 Pa, 25°C).

### 2.3.3 | Determination of tensile strength (TS) and elongation at break (E)

The film was cut into dimensions of 10 mm × 90 mm and subjected to tensile testing using a tensile machine (C42, MTS) at a speed of 100 mm/min.

### 2.3.4 | Antioxidant activity

The DPPH radical scavenging activity was used to assess the antioxidant activity of the films. The experiment was conducted with slight modifications based on the method described by Liu et al. (2023). Initially, 1 mL of anhydrous ethanol was mixed with 3 mL of a 0.2 mmol/L DPPH solution and kept away from light for 30 min. The absorbance was then measured at 517 nm and recorded as  $A_0$ . The procedure was repeated with 1 mL of the film solution in place of anhydrous ethanol to obtain the absorbance  $A_1$ . Additionally, 1 mL of the film solution was mixed with 3 mL of anhydrous ethanol to measure the absorbance  $A_2$ . The DPPH radical scavenging rate was calculated using the following formula:

$$DPPH \text{ radical scavenging rate} = \frac{A_0 - (A_1 - A_2)}{A_0} \times 100\%$$

### 2.3.5 | Antimicrobial ability

An inoculation loop was used to transfer a sample from slant-cultured strains into 3 mL of BHI fluid medium, which was then incubated in a constant temperature shaking incubator (DHP9082, YiHeng Scientific Instrument). The specific strains and incubation conditions are detailed in Table 1.

Following the method described by Zhang et al. (2022), 100 µL of activated bacterial or fungal suspension was spread evenly on solid media. Sterilized Oxford cups were placed vertically on the media. Each cup was filled with 200 µL of the following solutions: 0.5 g/L CS-ONP film solution, 1 g/L CS-ONP film solution, 0.5 g/L ONP solution, 1 g/L ONP solution, saline solution (negative control), 0.5 g/L streptomycin (positive control for bacteria), and 0.5 g/L fungicidin (positive control for fungi). Post-incubation, the inhibition zones were measured, and the data were recorded.

Bacterial and fungal suspensions were diluted to 10<sup>5</sup>–10<sup>6</sup> CFU/mL. A mixture of 100 µL of the diluted suspension, 2 mL of ONP solution at different concentrations and 15 mL of BHI fluid medium was incubated in a conical flask. Subsequently, 100 µL of the culture solution was taken, and the optical density (OD value) was measured at 517 nm. The concentration of ONP solution that resulted in an OD value of 0 was determined as the minimum inhibitory concentration.

### 2.3.6 | Chemical structure of the films

The chemical structure of the films was analyzed using Fourier Transform Infrared Spectroscopy (FT-IR)

**TABLE 1** Species of strains, culture conditions, and antimicrobial ability of onion polysaccharide (ONP) solutions and chitosan-ONP (CS-ONP) film solutions.

No.	Strain	Cate gory	Culture conditions	Inhibition zone diameter (mm)					PC	NC
				0.5 g/L ONP solution	1 g/L ONP solution	0.5 g/L CS-ONP film solution	1 g/L CS-ONP film solution			
1	<i>Escherichia coli</i>	Gram−	37°C, 12 h	9.07 ± 0.32* <sup>#</sup>	10.69 ± 0.33	9.22 ± 0.22* <sup>#</sup>	10.34 ± 0.41	10.16 ± 0.32	—	
2	<i>Pseudomonas aeruginosa</i>	Gram−	37°C, 12 h	8.39 ± 0.46* <sup>#</sup>	10.37 ± 0.33 <sup>#</sup>	8.93 ± 0.20*	10.31 ± 0.75 <sup>#</sup>	9.46 ± 0.64	—	
3	<i>Bacillus subtilis</i>	Gram+	37°C, 12 h	7.01 ± 0.04* <sup>#</sup>	8.46 ± 0.60 <sup>#</sup>	7.09 ± 0.15* <sup>#</sup>	8.59 ± 0.13 <sup>#</sup>	9.71 ± 0.40	—	
4	<i>Bacillus cereus</i>	Gram+	37°C, 12 h	7.07 ± 0.11* <sup>#</sup>	8.64 ± 0.36 <sup>#</sup>	7.21 ± 0.11* <sup>#</sup>	8.80 ± 0.46 <sup>#</sup>	9.80 ± 0.17	—	
5	<i>Aspergillus flavus</i>	Fungi	30°C, 48 h	9.50 ± 0.07*	10.31 ± 0.19 <sup>#</sup>	9.58 ± 0.26*	10.58 ± 0.47 <sup>#</sup>	9.32 ± 0.83	—	
6	<i>Aspergillus niger</i>	Fungi	30°C, 48 h	9.41 ± 0.44* <sup>#</sup>	10.29 ± 0.65	9.71 ± 0.27* <sup>#</sup>	10.46 ± 0.60	10.02 ± 0.74	—	
7	<i>Botrytis cinerea Pers.</i>	Fungi	30°C, 48 h	10.18 ± 0.42* <sup>#</sup>	11.26 ± 0.50	10.08 ± 0.34* <sup>#</sup>	11.44 ± 0.69	11.36 ± 0.87	—	
8	<i>Penicillium expansum</i>	Fungi	30°C, 48 h	9.75 ± 0.49* <sup>#</sup>	10.88 ± 0.13	10.00 ± 0.27* <sup>#</sup>	10.77 ± 0.43	11.06 ± 1.55	—	

Note: “\*” represents a significant statistical difference between the 0.5 g/L group and its corresponding 1 g/L group ( $p < 0.05$ ). “#” represents a significant statistical difference between this group and its corresponding positive control group ( $p < 0.05$ ). “—” represents the absence of an inhibition zone.

(Nicolet iS10, Thermo Fisher Scientific) to detect the functional groups present in the films. Prior to testing, the films were cut into 20 mm × 20 mm samples and analyzed using the Attenuated Total Reflectance mode of the FT-IR spectrometer. The interactions between substances were inferred by analyzing the characteristic peaks identified in the FT-IR spectra.

### 2.3.7 | Microstructure of the films

The microstructure of the films was examined using scanning electron microscopy (SEM). Prior to testing, the films were thoroughly dried and then cryo-fractured in liquid nitrogen. The films were cut into 1 mm × 6 mm samples, mounted on metal stubs, and sputter-coated with gold under vacuum. The morphology was observed using a Gemini 500 SEM (Carl Zeiss AG) at an accelerating voltage of 2.0 kV.

## 2.4 | Preservation experiment methods

### 2.4.1 | Treatment and storage conditions

A total of 240 fresh cherry tomatoes, uniform in size and shape, were randomly divided into six groups of 40 each. The blank group was untreated, whereas the control group used 0 g/L CS films. The other groups used 0.5, 1, 1.5, and 2 g/L CS-ONP composite films. Each cherry tomato was individually wrapped. Cherry tomatoes were stored at room temperature (25°C) for up to 16 days, with measurements taken on Days 0, 4, 8, 12, and 16. Measurement of the sample indicators began at 8:00 a.m. each day.

### 2.4.2 | Weight loss rate

Following Haile (2018), the initial weight was recorded on Day 0. Final weights were noted on Days 4, 8, 12, and 16. The weight loss rate was calculated as follows:

$$\text{Weight loss rate (\%)} = \frac{\text{initial weight} - \text{final weight}}{\text{initial weight}} \times 100\%$$

### 2.4.3 | Firmness

The firmness of cherry tomatoes was measured using a fruit firmness tester (GY-4, AiDebao Instrument) with a 4 mm diameter probe. The measurement was stopped when the probe penetrated 10 mm into cherry tomatoes, and the data were recorded. Measurements were taken at three points per cherry tomato, and the average was calculated.

### 2.4.4 | Total soluble solids (TSS) content

The content of total soluble solid (TSS) in cherry tomatoes was determined using a handheld refractometer (PAL-1, ATAGO). A sample of 5 g of cherry tomato fruit was ground in a mortar and centrifuged at 4000 rpm for 10 min (3K30 centrifuge, Sigma Laborzentrifugen GmbH), and the juice obtained was used for the measurement.

### 2.4.5 | Titratable acidity (TA) content

10 g of cherry tomato was ground, transferred to a 100 mL volumetric flask with distilled water, mixed, settled for

30 min, and filtered. The filtrate was titrated with 0.1 mol/L NaOH using phenolphthalein as an indicator to determine titratable acidity (TA) content.

#### 2.4.6 | Ascorbic acid (vitamin C) content

The ascorbic acid content in cherry tomatoes was determined using the 2,6-dichlorophenolindophenol titration method (Sumalan et al., 2020). Ten grams of cherry tomato was ground with 20 g/L oxalic acid, transferred to a 100 mL volumetric flask, mixed, settled for 10 min, and filtered. The filtrate was titrated with 0.1 g/L 2,6-dichlorophenolindophenol to determine ascorbic acid content.

#### 2.4.7 | Malondialdehyde (MDA) content

Following Hu et al. (2021), 1 g of cherry tomato was ground with 5 mL of 100 g/L trichloroacetic acid solution under ice bath conditions, centrifuged at 4°C and 10,000 × g for 20 min. The supernatant was mixed with 2 mL of 0.67% thiobarbituric acid solution, boiled, cooled, centrifuged, and absorbance was measured at 450, 532, and 600 nm.

### 2.5 | Statistical analysis

All experiments were repeated at least three times. Data are presented as mean ± SE. Statistical analysis was performed using SPSS version 27.0 (SPSS Inc.). One-way ANOVA determined significance, with  $p < 0.05$  considered significant. Graphs were generated using GraphPad Prism version 10.0 (GraphPad Software).

## 3 | RESULTS AND DISCUSSION

### 3.1 | Determination results of film properties

#### 3.1.1 | Thickness, color difference ( $\Delta E$ ), and transmittance (T)

As shown in Figure 1a, the addition of ONP resulted in only minor fluctuations in the thickness of the composite films, with no significant changes observed ( $p > 0.05$ ).

Figure 1b illustrates that the values of  $b^*$  and  $\Delta E$  gradually increased with the addition of ONP, indicating a color change in the composite films from light yellow to dark yellow, which is corroborated by Figure 1d.

Figure 1c shows that the increase in color difference led to a decrease in transmittance, suggesting that the

low transmittance of CS-ONP composite films effectively reduces the effect of light on the encapsulated material.

#### 3.1.2 | Moisture content (MC), swelling degree (SD), water solubility (WS), and water vapor permeability (WVP)

Figure 2a indicates that CS films without ONP had the highest moisture content (MC), which is closely related to the stable and highly functional CS-CS polymers that effectively reduce water evaporation during the drying process (Ahmed & Ikram, 2016; Choi et al., 2023). The addition of ONP disrupted this stability, forming less stable CS-ONP polymers, leading to exposure of water molecules in the film matrix and loss during drying. However, when ONP exceeded 1.5 g/L, the MC increased again due to the water affinity of ONP molecules and their surface adherence to CS-CS polymers. This trend was mirrored in the SD of the composite films, as shown in Figure 2b. The water solubility of composite films increased with ONP addition (Figure 2c), due to the lower molecular weight and polymerization degree of CS-ONP polymers compared to CS-CS polymers, and the water-soluble nature of ONP (Xu, Nie, et al., 2019).

Figure 2d shows that WVP was higher in 0 g/L CS films and 0.5 g/L CS-ONP composite films due to high MC. Compared to 0.5 g/L CS-ONP composite films, 1 and 1.5 g/L CS-ONP composite films had lower WVP. This was because, with the increase of the added amount, some ONP adhered to CS-CS polymers, and a large number of water vapor molecules were bound by them in the film matrix. Another reason was that 1 and 1.5 g/L CS-ONP composite films had lower MC. The combination of strong moisture binding capacity and high MC resulted in 2 g/L CS-ONP composite films with low WVP.

#### 3.1.3 | Tensile strength (TS) and elongation at break (E)

Figure 3a,b shows that both tensile strength and E decreased with increasing ONP addition. This is attributed to the formation of less stable CS-ONP polymers and the presence of non-polysaccharide substances in ONP that generate repulsive forces and reduce intermolecular interactions (Choi et al., 2023; Liu et al., 2023).

#### 3.1.4 | Antioxidant activity

Figure 3c illustrates that 0 g/L CS films exhibited weak antioxidant effects without ONP. The antioxidant capacity significantly improved with increased ONP addition.

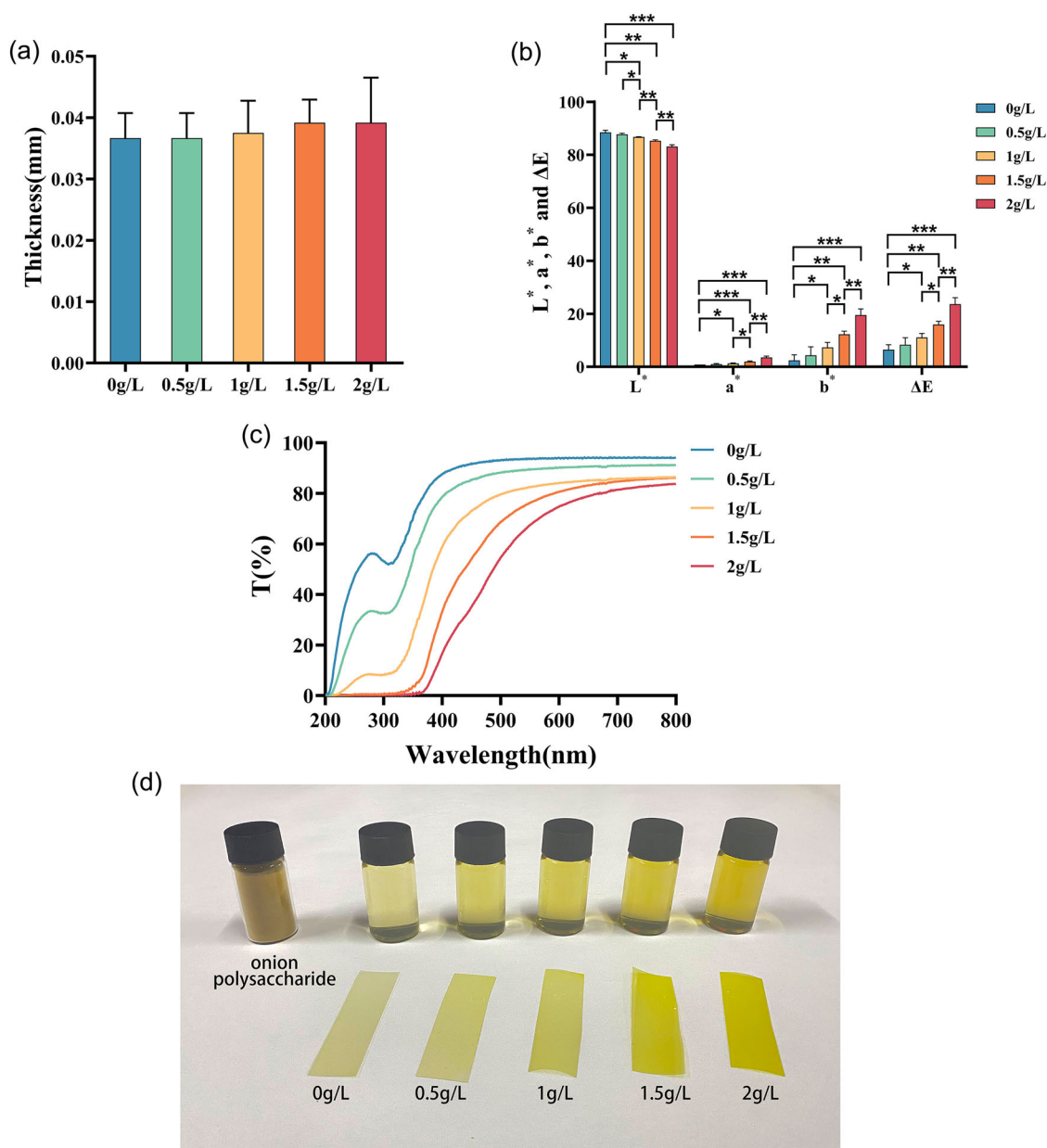


**FIGURE 1** Performance parameters of chitosan-onion polysaccharide (CS-ONP) composite films at different concentrations: (a) thickness, (b) color difference, (c) light transmittance, and (d) photographs of ONP, film solution, and composite films. Different colored columns and lines represent different concentrations of CS-ONP composite films. \* $p < 0.05$ , \*\* $p < 0.01$ , \*\*\* $p < 0.001$ .

### 3.1.5 | Antimicrobial activity

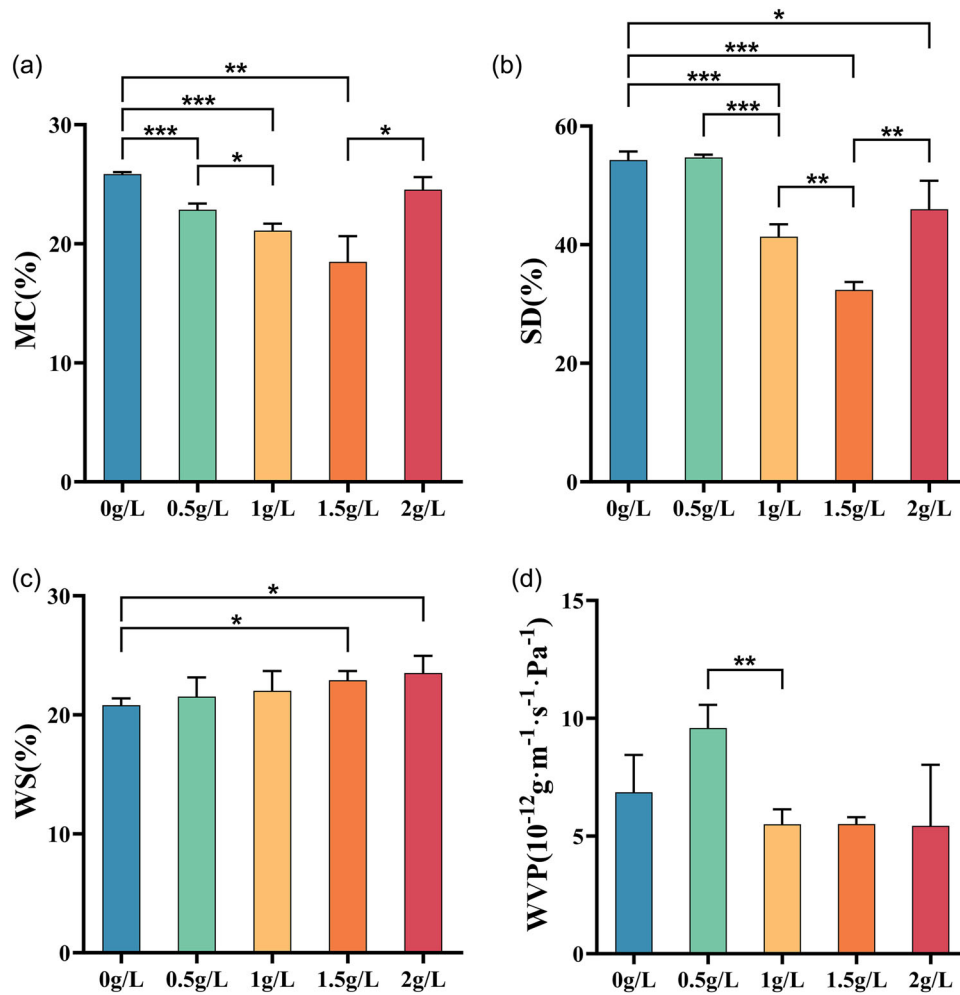
Plant polysaccharides disrupt microbial cell membranes and walls, affect RNA transcription, and hinder invasion (Li, Zhang, et al., 2022; Li, Han, et al., 2022).

Table 1 shows that 0.5 and 1 g/L ONP and CS-ONP solutions had good inhibitory effects against eight strains, with higher inhibition at 1 g/L. Notably, 1 g/L ONP showed better inhibition than the positive control for certain strains, suggesting ONP's potential as an antimicrobial substance.

Table 2 indicates that ONP had the best inhibitory effect on *B. cinerea Pers.*, requiring only 0.25 g/L for complete inhibition, whereas it was least effective against *B. subtilis* and *B. cereus*, needing 1 g/L for inhibition.

### 3.1.6 | Chemical structure

Figure 3d presents the FT-IR spectra of composite films with varying ONP concentrations. The broad absorption band near  $3353\text{ cm}^{-1}$  was associated with the stretching vibrations of O-H combined with N-H. The characteristic



**FIGURE 2** Performance parameters of chitosan-onion polysaccharide (CS-ONP) composite films at different concentrations: (a) moisture content, (b) swelling degree, (c) water solubility, and (d) water vapor permeability rate. Different colored columns represent different concentrations of CS-ONP composite films. \* $p < 0.05$ , \*\* $p < 0.01$ , \*\*\* $p < 0.001$ .

**TABLE 2** Minimum inhibitory concentration of onion polysaccharide (ONP) solution.

No.	Strain	2 g/L	1 g/L	0.5 g/L	0.25 g/L	0.125 g/L	0.0625 g/L
1	<i>Escherichia coli</i>	–	–	–	+	++	+++
2	<i>Pseudomonas aeruginosa</i>	–	–	–	+	+++	+++
3	<i>Bacillus subtilis</i>	–	–	+	++	++	+++
4	<i>Bacillus cereus</i>	–	–	+	++	++	+++
5	<i>Aspergillus flavus</i>	–	–	–	+	+	++
6	<i>Aspergillus niger</i>	–	–	–	+	+	++
7	<i>Botrytis cinerea Pers.</i>	–	–	–	–	+	++
8	<i>Penicillium expansum</i>	–	–	–	+	+	++

Note: “–” represents no bacterial growth, “+” represents bacterial growth.

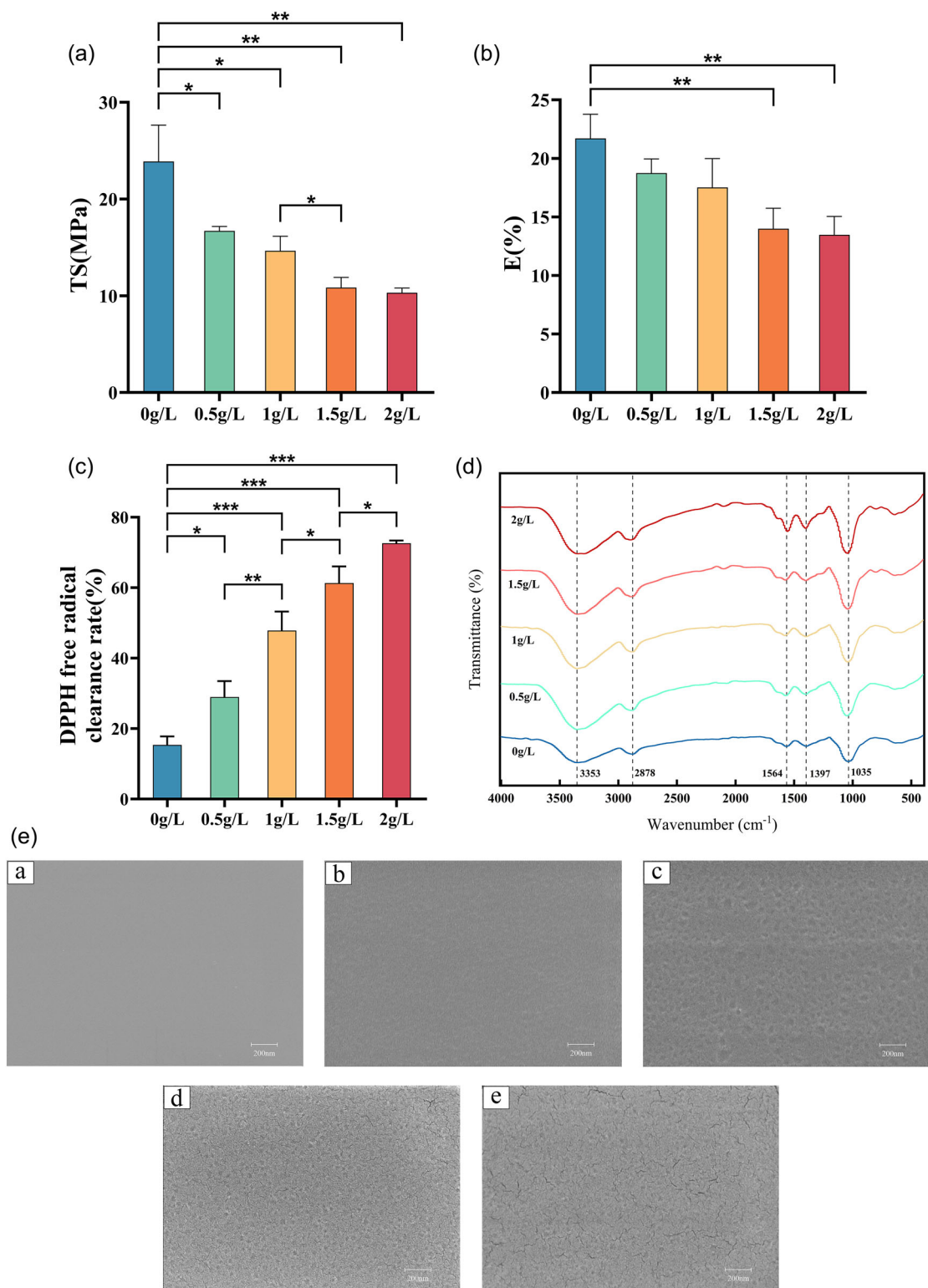


**FIGURE 3** Performance parameters of chitosan-onion polysaccharide (CS-ONP) composite films at different concentrations: (a) tensile strength, (b) elongation at break, (c) DPPH radical scavenging rate, (d) Fourier transform infrared (FT-IR) spectra, and (e) scanning electron microscopy (SEM) images: (a) 0 g/L CS films, (b) 0.5 g/L CS-ONP composite films, (c) 1 g/L CS-ONP composite films, (d) 1.5 g/L CS-ONP composite films, and (e) 2 g/L CS-ONP composite films. Different colored columns and lines represent different concentrations of CS-ONP composite films. \* $p < 0.05$ , \*\* $p < 0.01$ , \*\*\* $p < 0.001$ .

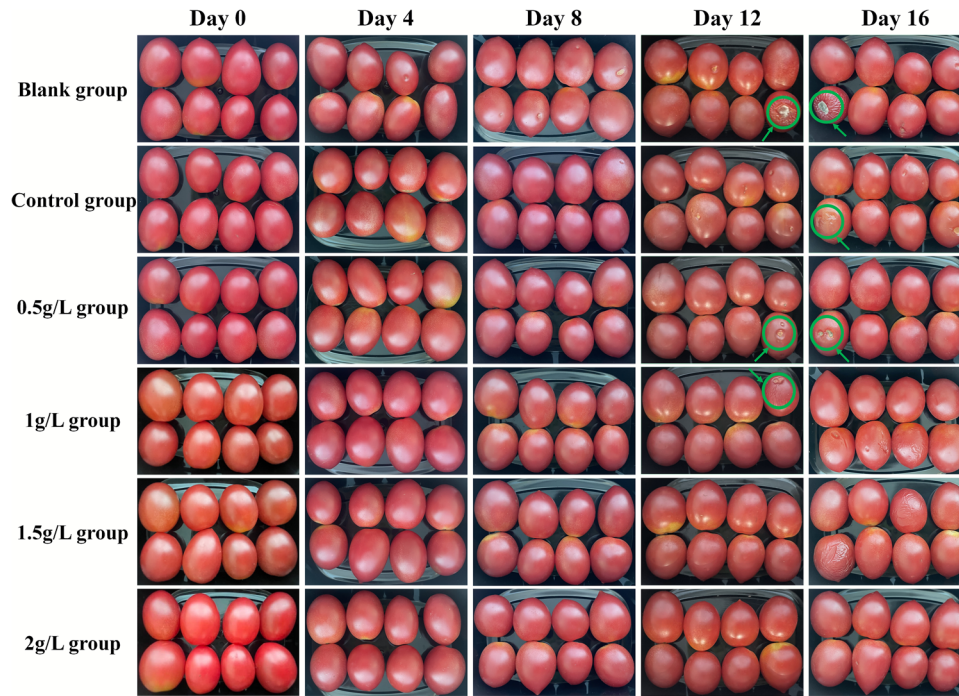


FIGURE 4 Physical pictures of cherry tomatoes on different days and groups.

peak at  $2878\text{ cm}^{-1}$  originated from the stretching vibration of  $-\text{CH}_2$ . The peak at  $1564\text{ cm}^{-1}$  was attributed to the bending vibration of  $\text{N}-\text{H}$ , and the peak at  $1397\text{ cm}^{-1}$  was due to the angular vibration of  $\text{C}-\text{H}$ . The peak around  $1035\text{ cm}^{-1}$  was likely linked to the stretching vibrations of  $\text{C}-\text{O}$  and  $\text{C}-\text{H}$  (Xiao et al., 2022). NO new absorption peaks appeared with ONP addition, but shifts in peak positions at  $1564$  and  $1035\text{ cm}^{-1}$  indicated electrostatic interactions and hydrogen bonding rather than chemical reactions between ONP and CS (Xu, Wei, et al., 2019).

### 3.1.7 | Microstructure

Figure 3e shows SEM images of composite films with varying ONP concentrations. The surface of films without ONP was smooth and flat (image a). With increasing ONP, the surface became wrinkled and uneven (images b and c), and higher ONP levels led to decreased stability and rough surfaces with localized cracking (images d and e).

## 3.2 | Preservation experiment results

### 3.2.1 | Weight loss rate

Transpiration and respiration caused significant water and organic matter loss in cherry tomatoes during storage (Zhang et al., 2019). Figure 5a shows that the blank group

had the highest weight loss rate after 16 days, whereas 0 g/L CS films suppressed weight loss only after 12 days. The addition of ONP advanced this effect to the 8th day. The 2 g/L CS-ONP composite films were most effective in retarding weight loss, although not significantly different from other CS-ONP composite films.

### 3.2.2 | Firmness

Figure 5b shows a decrease in firmness, related to pectin decomposition in cherry tomatoes. The 2 g/L CS-ONP composite films best inhibited firmness loss, followed by 1.5, 1, and 0.5 g/L groups. Figure 4 shows the appearance of spots and rotting starting from Day 12 in blank, control, 0.5 and 1 g/L groups.

### 3.2.3 | TSS content

Figure 5c shows that TSS content initially increased then decreased, influenced by carbohydrate metabolism (Hu et al., 2012; Zhou et al., 2013). The highest TSS content was on Day 4 for blank and control groups, and on Day 8 for CS-ONP groups. After 16 days, the 1, 1.5, and 2 g/L groups maintained high TSS content, with 2 g/L being the highest, indicating that CS-ONP composite films effectively preserved TSS (Gol et al., 2013).

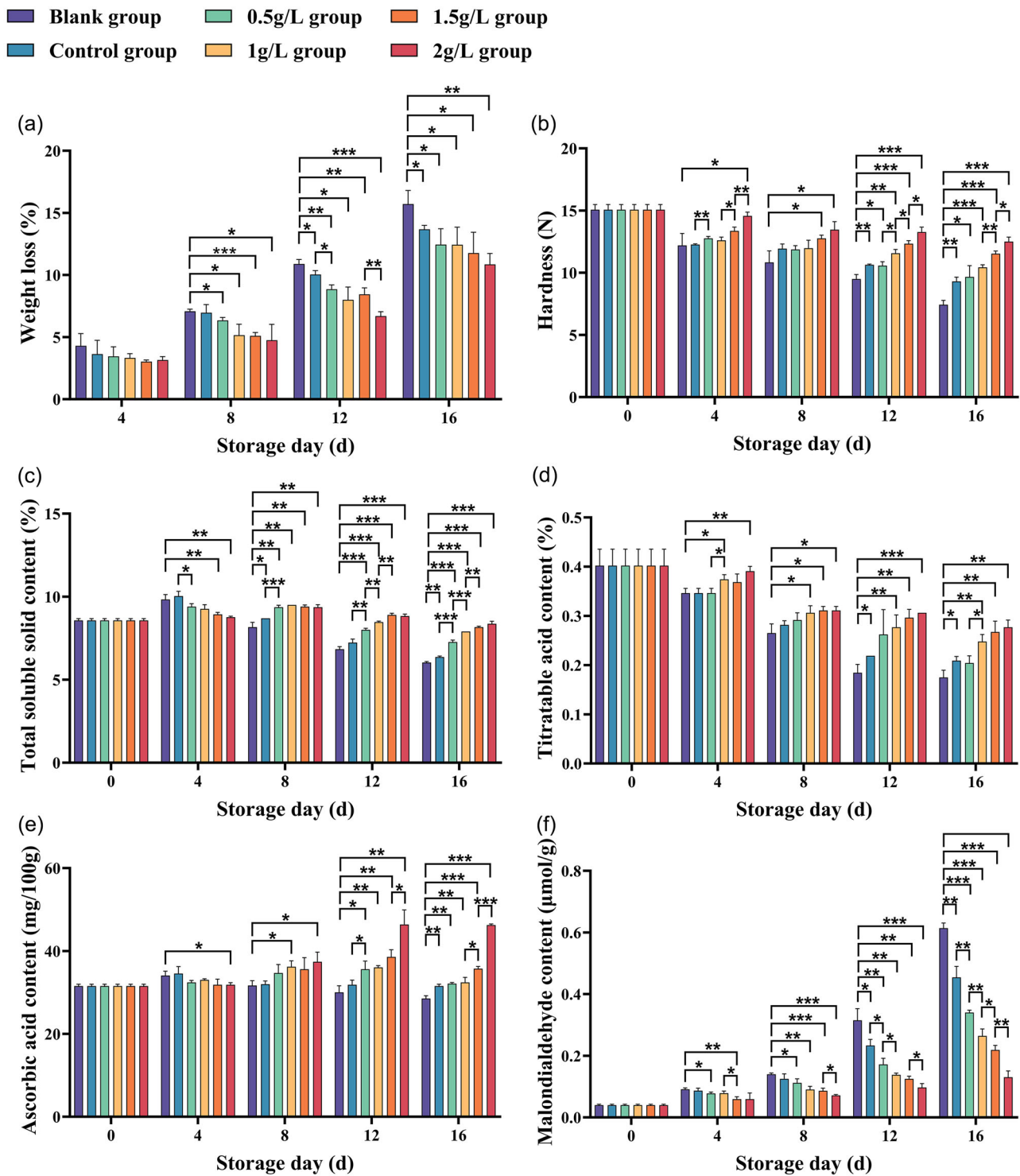


FIGURE 5 Effectiveness indicators of chitosan-onion polysaccharide (CS-ONP) composite films at different concentrations on the preservation of cherry tomatoes: (a) weight loss rate, (b) firmness, (c) total soluble solids content, (d) titratable acidity content, (e) ascorbic acid content, and (f) malondialdehyde content. Different colored columns represent different concentrations of CS-ONP composite films. \* $p < 0.05$ , \*\* $p < 0.01$ , \*\*\* $p < 0.001$ .

### 3.2.4 | TA content

Malic and citric acids were two main organic acids contained in cherry tomatoes and were important influences on the flavor of cherry tomatoes (Lai et al., 2022). Figure 5d shows a decrease in TA content due to organic acid conversion during post-ripening (Al-Dairi et al., 2021; Yeshiwas & Tolessa, 2018). The blank group had the fastest decrease, whereas 1, 1.5, and 2 g/L groups maintained higher TA from Days 8–16.

### 3.2.5 | Ascorbic acid content

Ascorbic acid content initially increased due to post-ripening and then decreased due to oxidation (Chen et al., 2023; Xiang et al., 2021), as shown in Figure 5e. The blank group had a gradual decrease after Day 4, whereas the control group had higher ascorbic acid on Day 16. CS-ONP composite films delayed the peak and maintained higher ascorbic acid content due to their antioxidant properties.

### 3.2.6 | MDA content

Malondialdehyde (MDA), a product of lipid peroxidation, increased during storage (Li et al., 2022), as shown in Figure 5f. The blank group had the highest increase due to direct air exposure. The control group's MDA content was lower but higher than CS-ONP groups. The 2 g/L CS-ONP composite films best inhibited MDA accumulation after 12 days.

## 4 | CONCLUSIONS

This study systematically examined the properties of CS-ONP composite films and their application in cherry tomato preservation. The addition of ONP improved the films' shading, antimicrobial, and antioxidant abilities while reducing mechanical properties and altering microstructure. Preservation tests showed that CS-ONP composite films effectively delayed the quality decline of cherry tomatoes during storage.

### AUTHOR CONTRIBUTIONS

**Ao Shen:** Conceptualization; data curation; formal analysis; writing—original draft; writing—review and editing. **Tianzhu Zhang:** Formal analysis; writing—original draft. **Shuzhen Li:** Project administration; resources; supervision; writing—review and editing. **Miaorong Xiao:** Methodology; writing—original draft. **Zhijun Tian:** Data curation; formal analysis. **Jin Zhang:** Formal analysis.

**Tongtong Lu:** Formal analysis. **Weiwei Yang:** Funding acquisition; methodology; project administration; supervision; writing—review and editing.

### ACKNOWLEDGMENTS

This work was supported by the Natural Science Foundation of Liaoning Province (2018010874-301, 2017225065) and Shenyang Medical College Scientific Research Innovation Fund (20182033, 20191038).

### CONFLICT OF INTEREST STATEMENT

The authors have declared no conflicts of interest for this article.

### ORCID

Weiwei Yang  <https://orcid.org/0000-0001-8286-8708>

### REFERENCES

- Abd El-Hack, M. E., El-Saadony, M. T., Shafi, M. E., Zaberawi, N. M., Arif, M., Batiha, G. E., Khafaga, A. F., Abd El-Hakim, Y. M., & Al-Sagheer, A. A. (2020). Antimicrobial and antioxidant properties of chitosan and its derivatives and their applications: A review. *International Journal of Biological Macromolecules*, 164, 2726–2744. <https://doi.org/10.1016/j.ijbiomac.2020.08.153>
- Ahmed, S., & Ikram, S. (2016). Chitosan and gelatin based biodegradable packaging films with UV-light protection. *Journal of Photochemistry & Photobiology, B: Biology*, 163, 115–124. <https://doi.org/10.1016/j.jphotobiol.2016.08.023>
- Al-Dairi, M., Pathare, P. B., & Al-Yahyai, R. (2021). Chemical and nutritional quality changes of tomato during postharvest transportation and storage. *Journal of the Saudi Society of Agricultural Sciences*, 20, 401–408. <https://doi.org/10.1016/j.jssas.2021.05.001>
- Chen, K., Tian, R. M., Xu, G. J., Wu, K., Liu, Y., & Jiang, F. T. (2023). Characterizations of konjac glucomannan/curdlan edible coatings and the preservation effect on cherry tomatoes. *International Journal of Biological Macromolecules*, 232, 123359. <https://doi.org/10.1016/j.ijbiomac.2023.123359>
- Choi, I., Lee, B. Y., Kim, S., Imm, S., Chang, Y., & Han, J. (2023). Comparison of chitosan and gelatin-based films and application to antimicrobial coatings enriched with grapefruit seed extract for cherry tomato preservation. *Food Science and Biotechnology*, 32(8), 1067–1077. <https://doi.org/10.1007/s10068-023-01254-9>
- Cohen, E., & Poverenov, E. (2022). Hydrophilic chitosan derivatives: Synthesis and applications. *Chemistry (Weinheim An Der Bergstrasse, Germany)*, 28(67), e202202156. <https://doi.org/10.1002/chem.202202156>
- de Morais Lima, M., Carneiro, L. C., Bianchini, D., Dias, A. R. G., Zavareze, E. D. R., Prentice, C., & Moreira, A. D. S. (2017). Structural, thermal, physical, mechanical, and barrier properties of chitosan films with the addition of xanthan gum. *Journal of Food Science*, 82(3), 698–705. <https://doi.org/10.1111/1750-3841.13653>
- Gol, N. B., Patel, P. R., & Rao, T. V. R. (2013). Improvement of quality and shelf-life of strawberries with edible coatings enriched with chitosan. *Postharvest Biology and Technology*, 85, 185–195. <https://doi.org/10.1016/j.postharvbio.2013.06.008>
- Haile, A. (2018). Shelf life and quality of tomato (*Lycopersicon esculentum* Mill.) fruits as affected by different packaging materials.

- African Journal of Food Science*, 12(2), 21–27. <https://doi.org/10.5897/ajfs2017.1568>
- Hu, E. M., Liu, M., Zhou, R., Jiang, F. L., Sun, M. T., Wen, J. Q., Zhu, Z. H., & Wu, Z. (2021). Relationship between melatonin and abscisic acid in response to salt stress of tomato. *Scientia Horticulturae*, 285, 110176. <https://doi.org/10.1016/j.scienta.2021.110176>
- Hu, L. Y., Hu, S. L., Wu, J., Li, Y. H., Zheng, J. L., Wei, Z. J., Liu, J., Wang, H. L., Liu, Y. S., & Zhang, H. (2012). Hydrogen sulfide prolongs postharvest shelf life of strawberry and plays an antioxidative role in fruits. *Journal of Agricultural and Food Chemistry*, 60(35), 8684–8693. <https://doi.org/10.1021/jf300728h>
- Kumari, N., Kumar, M., Radha, Lorenzo, J. M., Sharma, D., Puri, S., Pundir, A., Dhumal, S., Bhuyan, D. J., Jayanthi, G., Selim, S., Abdel-Wahab, B. A., Chandran, D., Anitha, T., Deshmukh, V. P., Pandiselvam, R., Dey, A., Senapathy, M., Rajalingam, S., ... Kennedy, J. F. (2022). Onion and garlic polysaccharides: A review on extraction, characterization, bioactivity, and modifications. *International Journal of Biological Macromolecules*, 219, 1047–1061. <https://doi.org/10.1016/j.ijbiomac.2022.07.163>
- Lai, Y. P., Wang, W. T., Zhao, J. J., Tu, S., Yin, Y. W., & Ye, L. Y. (2022). Chitosan Na-montmorillonite films incorporated with citric acid for prolonging cherry tomatoes shelf life. *Food Packaging and Shelf Life*, 33, 100879. <https://doi.org/10.1016/j.foodchem.2022.100879>
- Li, M., Zhang, H. N., Hu, X. Y., Liu, Y. M., Liu, Y. F., Song, M. J., Wu, R. N., & Wu, J. R. (2022). Isolation of a new polysaccharide from dandelion leaves and evaluation of its antioxidant, antibacterial, and anticancer activities. *Molecules (Basel, Switzerland)*, 27(21), 7641. <https://doi.org/10.3390/molecules27217641>
- Li, Y., Han, L. X., Wang, B. B., Zhang, J., & Nie, J. Y. (2022). Dynamic degradation of penconazole and its effect on antioxidant enzyme activity and malondialdehyde content in apple fruit. *Scientia Horticulturae*, 300, 111053. <https://doi.org/10.1016/j.scienta.2022.111053>
- Liu, W. L., Kang, S., Zhang, Q. S., Chen, S., Yang, Q., & Yan, B. (2023). Self-assembly fabrication of chitosan-tannic acid/MXene composite film with excellent antibacterial and antioxidant properties for fruit preservation. *Food Chemistry*, 410, 135405. <https://doi.org/10.1016/j.foodchem.2023.135405>
- Matica, M. A., Aachmann, F. L., Tøndervik, A., Sletta, H., & Ostafe, V. (2019). Chitosan as a wound dressing starting material: Antimicrobial properties and mode of action. *International Journal of Molecular Sciences*, 20(23), 5889. <https://doi.org/10.3390/ijms20235889>
- Shen, A., Zhang, T. Z., Li, S. Z., Zhou, X. Q., Xiao, M. R., Chen, X. D., Zhang, B. W., & Yang, W. W. (2023). Beneficial effects of *Pleurotus citrinopileatus* polysaccharide on the quality of cherry tomatoes during storage. *Foodborne Pathogens and Disease*, 20(9), 398–404. <https://doi.org/10.1089/fpd.2023.0032>
- Sumalan, R. M., Ciulca, S. I., Poiana, M. A., Moigradean, D., Radulov, I., Negrea, M., Crisan, M. E., Copolovici, L., & Sumalan, R. L. (2020). The antioxidant profile evaluation of some tomato landraces with soil salinity tolerance correlated with high nutraceutical and functional value. *Agronomy*, 10(4), 500. <https://doi.org/10.3390/agronomy10040500>
- Wilson, L. A., Delige, F., Wang, T., & Cosgrove, D. J. (2021). Saccharide analysis of onion outer epidermal walls. *Biotechnology for Biofuels*, 14(1), 66. <https://doi.org/10.1186/s13068-021-01923-z>
- Xiang, F., Xia, Y. T., Wang, Y., Wang, Y. X., Wu, K., & Ni, X. W. (2021). Preparation of konjac glucomannan based films reinforced with nanoparticles and its effect on cherry tomatoes preservation. *Food Packaging and Shelf Life*, 29, 100701. <https://doi.org/10.1016/j.foodchem.2021.100701>
- Xiao, L. Q., Kang, S., Lapu, M., Jiang, P., Wang, X. H., Liu, D. Y., Li, J., & Liu, M. X. (2022). Preparation and characterization of chitosan/pullulan film loading carvacrol for targeted antibacterial packaging of chilled meat. *International Journal of Biological Macromolecules*, 211, 140–149. <https://doi.org/10.1016/j.ijbiomac.2022.05.044>
- Xu, C. H., Nie, J. D., Wu, W. C., Zheng, Z. J., & Chen, Y. K. (2019). Self-healable, recyclable, and strengthened epoxidized natural rubber/carboxymethyl chitosan bio-based composites with hydrogen bonding supramolecular hybrid network. *ACS Sustainable Chemistry & Engineering*, 7(18), 9b04324. <https://doi.org/10.1021/acssuschemeng.9b04324>
- Xu, J. H., Wei, R. B., Jia, Z., & Song, R. (2019). Characteristics and bioactive functions of chitosan/gelatin-based film incorporated with  $\epsilon$ -polylysine and astaxanthin extracts derived from by-products of shrimp (*Litopenaeus vannamei*). *Food Hydrocolloids*, 100, 105436. <https://doi.org/10.1016/j.foodhyd.2019.105436>
- Yeshiwas, Y., & Tolessa, K. (2018). Postharvest quality of tomato (*Solanum lycopersicum*) varieties grown under greenhouse and open field conditions. *International Journal of Biotechnology and Molecular Biology Research*, 9(1), 1–6. <https://doi.org/10.5897/IJBMBR2015.0237>
- Zhang, J. H., Cui, X., Zhang, M., Bai, B. Q., Yang, Y. K., & Fan, S. H. (2022). The antibacterial mechanism of perilla rosmarinic acid. *Biotechnology and Applied Biochemistry*, 69(4), 1757–1764. <https://doi.org/10.1002/bab.2248>
- Zhang, X. T., Zhang, X. L., Liu, X. C., Du, M. L., & Tian, Y. Q. (2019). Effect of polysaccharide derived from *Osmunda japonica* Thunb-incorporated carboxymethyl cellulose coatings on preservation of tomatoes. *Journal of Food Processing and Preservation*, 42(12), e14239. <https://doi.org/10.1111/jfpp.14239>
- Zhou, H. M., Jia, N., Zhang, H. X., Xie, Y. H., Liu, H., Kong, B. H., & Luo, Y. B. (2013). Study on antifungal properties of bacteriocin produced by *Lactobacillus* and application in fruit preservation. *Advanced Materials Research*, 781, 1315–1321. <https://doi.org/10.4028/www.scientific.net/AMR.781-784.1315>
- Zhou, N., Zhao, Y., Zhang, L. G., & Ning, Y. B. (2022). Protective effects of black onion polysaccharide on liver and kidney injury in T2DM rats through the synergistic impact of hypolipidemic and antioxidant abilities. *International Journal of Biological Macromolecules*, 223(Pt A), 378–390. <https://doi.org/10.1016/j.ijbiomac.2022.11.055>
- Zhou, S. Y., Huang, G. L., & Huang, H. L. (2022). Extraction, derivatization and antioxidant activities of onion polysaccharide. *Food Chemistry*, 388, 133000. <https://doi.org/10.1016/j.foodchem.2022.133000>

**How to cite this article:** Shen, A., Zhang, T., Li, S., Xiao, M., Tian, Z., Zhang, J., Lu, T., & Yang, W. (2024). Innovative chitosan-onion polysaccharide composite films: A study on the preservation effects on cherry tomatoes. *Journal of Food Science*, 1–13. <https://doi.org/10.1111/1750-3841.17262>